

# Hydrothermal Behavior of G-S Magnetically Stabilized Beds Consisting of Magnetic and Non-Magnetic Admixtures

Z. Al-Qodah, M. Al-Busoul, and A. Khraewish

**Abstract**—The hydrothermal behavior of a bed consisting of magnetic and shale oil particle admixtures under the effect of a transverse magnetic field is investigated. The phase diagram, bed void fraction are studied under wide range of the operating conditions i.e., gas velocity, magnetic field intensity and fraction of the magnetic particles. It is found that the range of the stabilized regime is reduced as the magnetic fraction decreases. In addition, the bed voidage at the onset of fluidization decreases as the magnetic fraction decreases. On the other hand, Nusselt number and consequently the heat transfer coefficient is found to increase as the magnetic fraction decreases. An empirical equation is investigated to relate the effect of the gas velocity, magnetic field intensity and fraction of the magnetic particles on the heat transfer behavior in the bed.

**Keywords**—Magnetic stabilization; Magnetic stabilized fluidized beds; Gas-fluidized beds.

## I. INTRODUCTION

SINCE their first large-scale application in chemical processing in the early 1920s, gas-fluidized beds have been developed into one of the main types of commercial reactors used to carry-out gas–solid reactions [1]. These reactors offer a number of potential advantages including isothermal conditions, low pressure drop and possibility to use small particles [2,3]. However, these reactors usually suffer from the presence of large gas bubbles causing low mass transfer between the two phases.

Magnetic stabilization of fluidized beds is a technology developed to eliminate the drawbacks of fluidized beds [4]. Many studies have realized that magnetic stabilized beds (MSBs) combine the most desirable characteristics of both fluidized and packed beds including low-pressure drops of fluidized beds with the bubble-free operation at high gas flow rates of packed beds [5]. For this reason, many studies have tried to exploit the unique advantages of MSBs in some chemical and biochemical processes in addition to some separation techniques [6].

Z. Al-Qodah is with Hashemite University, Director of the Center of Environmental Studies, Zarka, 13115, P. O. Box 330127, Jordan (phone: +962777487890, fax: +96253823348, e-mail: zak@hu.edu.jo, zakaria\_al\_qodah@fet.edu.jo).

M. Al-Busoul is with Department of Mechanical Engineering and A. Khraewish is with Department of Electrical Engineering, Faculty of Engineering Technology, Al-Balqa Applied University, Mark, P. O. Box 15008, Amman, Jordan.

A further possible application of magnetic stabilization technology is to improve the performance of combustion reactors of some solid fossil fuels such as shale oil, which represents a promising source of energy in 31 countries including Jordan [7]. However, magnetic stabilization implies suppression of the solid phase mixing movements in the magnetic bed. This effect usually reduces the heat transfer coefficient across the bed and could represent a major restriction to apply this approach on highly exothermic processes.

Fortunately, the use of admixtures of magnetic particles with non-magnetic particles of shale oil for instance in a combustor utilizing a magnetic field could improve its performance by overtaking the stabilization drawbacks. In one hand, the stabilized combustor could operate with higher gas flow rates without particles washout in addition to the effect of the magnetic field in suppressing bubble formation in the bed [8]. Furthermore, the use of non-magnetic particles beside the magnetic particles in magnetically stabilized beds is expected to enhance the solid phase mixing movements which consequently increases the heat transfer coefficient. In addition the use of these admixtures could reduce the bed weight and consequently the pressure drop across the bed and could reduce the magnetic particles aggregation [9].

The hydrodynamics of G-S magnetic stabilized beds utilizing admixtures of magnetic and non-magnetic particles has been studied by several authors [9-12]. In contrast, few studies dealing with heat transfer characteristics in such systems have been cited in the literature [13,14]. In these studies it was shown that bed magnetic stabilization was obtained even with low mass fraction of the magnetic particles. However, it was reported that the bed fluidization behavior and the stability diagram change strongly as the non-magnetic mass fraction increases [9,13]. Moreover, Ganzha and Saxena [14] reported that the hydrodynamic and thermal behavior in these systems is affected by the bed voidage, mass fraction and segregation of the admixture particles.

In view of the promising economic value of the shale oil reserves in Jordan and the efforts to explore these reserves as a new energy source either by direct combustion or by retorting, G-S magnetically stabilized beds containing admixtures of magnetic and non-magnetic particles could be considered as a good candidate contactor to carry out shale oil processes. For this reason, the aim of this study was directed to investigate the thermal behavior of this system under the effect of transverse magnetic field. Experiments have been conducted using admixture made of shale oil

particles and magnetic particles. The effect of the magnetic portion in the mixture, gas velocity and magnetic field intensity on the mass transfer coefficient was investigated.

## II. EXPERIMENTAL

### A. Experimental Setup and Materials

A schematic diagram of the experimental apparatus is shown in Fig. 1. The column is constructed from transparent Plexiglas pipe to facilitate visual observations. The column height is 0.9 m with 0.07-m I.D and 4 mm thick. At the base of the column, a stainless steel non-magnetic grid of 0.33-mm whole diameter is used to support the solid phase bed, which is 0.13 m height.

Fig. 1 (inset 13) shows the details of the heating system used in the net surface area of the heater are  $7.068 \times 10^{-4} \text{ m}^2$ , and the total volume of the heater with its arm is  $2.557 \times 10^{-6} \text{ m}^3$ . The input electrical power of the heater, IV, is constant and is equal to 7 W. The heater was located in the center of the bed 0.07 m above the supporting grid.

The magnetic particles used in this investigation are prepared in the same manner as described earlier [16]. More details about the magnetic system, heating system and magnetic particles are found elsewhere [1, 15, 16]. The shale oil particles are obtained from the Authority of Natural resources, Amman, Jordan. Samples were crushed and dried then classified into different fractions. Some properties of the magnetic particles and shale oil particles used in this investigation are shown in Table I, where  $\rho_b$  and  $\rho_s$  are the bulk and solid densities ( $\text{kg/m}^3$ ), respectively,  $d_p$ , particles diameter (mm),  $U_{mfo}$ , minimum fluidization velocity in the absence of the magnetic field,  $B_s$ , saturation magnetic field intensity (m T), and  $C_p$  is the heat capacity (J/kg.K).

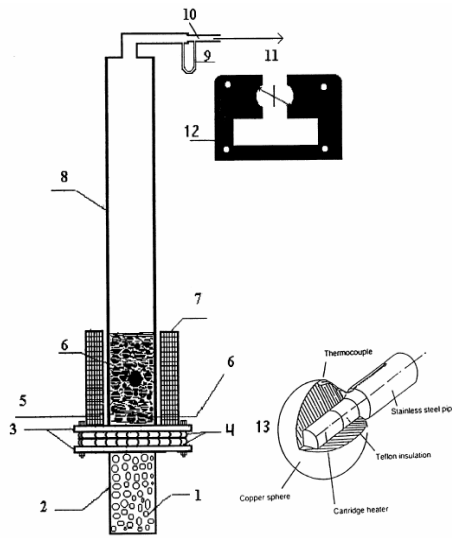


Fig. 1 Schematic of the experimental setup: 1 gas entrance, 2 polyethylene particles, 3 flanges, 4 supporting grid, 5 heater, 6 magnetic particles, 7 magnetic system, 8 column, 9 manometer, 10 orifice, 11 gas suction, 12 details of the magnetic sheets, and 13 details of the heater

TABLE I  
CHARACTERISTICS OF THE SOLID PHASE PARTICLES USED

| Type | $\rho_b$<br>( $\text{kg/m}^3$ ) | $\rho_s$<br>( $\text{kg/m}^3$ ) | $d_p$<br>(mm) | $U_{mfo}$<br>(m/s) | $B_s$<br>(m T) | $\epsilon_0$ (-) | $C_p$<br>(J/kg) |
|------|---------------------------------|---------------------------------|---------------|--------------------|----------------|------------------|-----------------|
| 1    | 1750                            | 3020                            | 0.9           | 0.574              | 590            | 0.42             | 362             |
| 2    | 1905                            | 3230                            | 1.0           | 0.690              | 590            | 0.41             | 370             |
| 3    | 870                             | 1500                            | 0.85          | 0.246              | ---            | 0.42             | 850             |

- 1 Activated carbon magnetic particles 1
- 2 Activated carbon magnetic particles 2
- 3 Shale oil non-magnetic particles

### B. Procedure

The mean diameter of the magnetic particles  $d_p$  is determined using the following formula proposed by Botterill [17]:

$$d_p = [\sum(x_i / d_{pi})]^{-1} \quad (1)$$

where  $x_i$  mass fraction (-).

The average density of the solid phase in the bed is calculated using the following equation [14]:

$$\rho_s = [(X_M / \rho_M) + \{(1 - X_M) / \rho_N\}]^{-1} \quad (2)$$

where  $X_M$  the mass fraction of the magnetic particles in the admixture (-),  $\rho_M$  and  $\rho_N$  the densities of the magnetic and shale oil particles ( $\text{kg/m}^3$ ).

The initial bed height is 0.10 m. The following equations are used to calculate the initial solid holdup,  $\epsilon_{so}$ , solid holdup after bed expansion,  $\epsilon_s$ , and the bed porosity,  $\epsilon$ , respectively:

$$\epsilon_{so} = \left(\frac{W}{\rho_s}\right) / (AH_{bo} - V_h) \quad (3)$$

$$\epsilon_s = 1 - \left(\frac{H_{bo}}{H_b}\right) \epsilon_{so} \quad (4)$$

$$\epsilon = 1 - \epsilon_s \quad (5)$$

where  $H_b$ ,  $H_{bo}$  are bed height and initial bed height (m),  $A$  cross sectional area ( $\text{m}^2$ ),  $W$  bed mass (kg),  $V_h$  is the heater volume  $\text{m}^3$ .

The effect of radiation heat transfer in this study is neglected. Temperature is measured with a copper constantan thermocouple. The readout of the temperature device gives directly the difference between the heater and the inlet gas temperature. Gas flow rate was measured using an orifice meter (Armfield, England) located on the line between the suction fan and the top of the column. The magnetic field intensity is measured using Hall probe (Leybold-Heraeus, Germany).

The heat transfer coefficient,  $h$  ( $\text{W/m}^2\text{K}$ ) is calculated using the following equation:

$$h = Q / [A(T_s - T_b)] = IV / A(T_s - T_b) \quad (6)$$

where  $Q$  power input (W),  $s$  heater surface area ( $\text{m}^2$ ),  $T_s$  and  $T_b$  are the temperatures of the heater surface and the bed (K),  $I$  current (Ampere),  $V$  applied voltage (Volts),  $C_p$  heat capacity (J/kg.K).

In this study, experiments were conducted in the mode of "Magnetizing first" which means that the magnetic field is set

at the desired value and applied to a static bed. After that, the gas flow is started. In this mode of operation and before starting to carry out each experiment, the bed is fluidized in the absence of the magnetic field for 3 min, followed by slow decrease of the gas flow down to the formation of the initial packed bed.

### III. RESULTS AND DISCUSSION

#### A. Hydrodynamic behavior of MSBs with Admixtures Phase Diagram

In magnetically stabilized beds, consisting of pure magnetic particles, the bed structure shows three subsequent flow regimes as the gas velocity increases, at constant magnetic field intensity: The initial packed bed, the magnetically stabilized expanded bed, and finally, the fluidized bed regime. The fluidized bed regime starts with a bubbling phase consisting of fluidized strings of particles and ends with a homogeneous fluidization of strings of particles. At the beginning of the magnetically stabilized regime the bed is characterized by its uniform structure of the chains of particles arranged in the direction of the field lines with the absence of cracks or cavities, whereas, at the end of this regime and the onset of the fluidized regime, the bed is characterized by the presence of cracks and horizontal slits if the field is horizontal and vertical channels if the field is axial [1, 15]. On the other hand, in magnetically stabilized beds, consisting of admixtures of magnetic and nonmagnetic magnetic and nonmagnetic particles, the magnetic particles tend to form layers or networks of stationary chains along the field lines. The nonmagnetic particles of the admixture are enclosed between these networks. While the magnetic particles in the networks are stabilized with no movements, the nonmagnetic particles in the cavity between the networks are fluidized or agitated and the intensity of their movements depend on both the gas velocity and the magnetic intensity. This behavior of the particles admixture in the bed is named ‘‘Bacon structure’’ [9, 18].

Fig. 2 shows an experimental phase diagram for two different fractions of the magnetic particles as a function of magnetic field intensity and gas superficial velocity. The solid lines represent the variation of  $U_e$  and  $U_{mf}$  of pure magnetic particles whereas the dashed lines represent the variation of these variables for a mixture of containing 75% magnetic particles. It is evident that in both mixtures the values of the minimum expansion velocity of the bed,  $U_e$  are approximately constant and close to that of  $U_{mf0}$  or the minimum fluidizing velocity in the absence of magnetic field. In contrast  $U_{mf}$  is found to increase as the magnetic field intensity increases. The experimental values of  $U_{mf}$  for certain admixture and those calculated by equation 6 as a function of magnetic field intensity,  $B$  are given in Table II. It could be noticed that good agreement between experimental and theoretical values at  $B < 30$  m T. At higher values of  $B$  the discrepancy increases may be because equation 6 does not consider the aggregation occurred to the magnetic particles at relatively high fields. The same phenomenon was reported by Ganzha and Saxena [14]. In addition, Fig. 2 reveals that as the

fraction of the magnetic particles decreases, both  $U_e$  and  $U_{mf}$  decreases. For example at  $B$  of 30 m T,  $U_e$  decreases from 0.574 to 0.553 m/s and  $U_{mf}$  decreases from 0.74 to 0.68 m/s as the mass fraction of the magnetic particles decreases from 100 to 75%. This is reasonable since the non magnetic particles have lower densities than the magnetic ones and the non magnetic particles reduce the effect of aggregation. Thivel *et al.*, (2004) reported that the both  $U_e$  and  $U_{mf}$  in the absence of magnetic field are not affected by the mass fraction of the magnetic particles. They showed graphically that at  $H$  value of 0 kA/m, both  $U_e$  and  $U_{mf}$  were equal 1.2 m/s for three different mass fractions of magnetic particles. The densities of the particles they used were 7000 and 2500 kg m<sup>-3</sup> for the magnetic and nonmagnetic particles, respectively. Accordingly, the density of their mixture sharply decreases as the mass fraction of the magnetic particles decreases. For this reason their results are not reasonable since both of  $U_e$  and  $U_{mf}$  decrease as the bed density decreases. The change in  $U_{mf}$  is more significant than the change in  $U_e$  since the presence of nonmagnetic particles could reduce the aggregation of the magnetic particles and consequently reduces the required pressure drop across the bed in order to fluidize the particles.

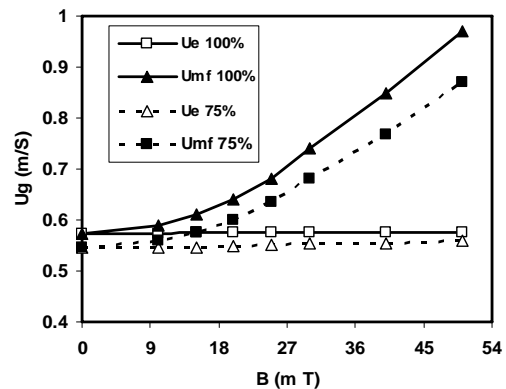


Fig. 2 Phase diagram of admixtures beds of magnetic and nonmagnetic particles under the effect of transverse magnetic field. \_\_\_\_\_ Pure magnetic particles, -----Admixture

#### Bed Expansion

Bed expansion is an important property of gas-solid systems. It affects the size of the fluid-bed equipment and residence time(s) of the fluid phase(s) and consequently affects the heat transfer rate in the bed [18, 19]. The height of the magnetized bed increases as the gas superficial velocity  $U_g$  exceeds the minimum expansion velocity,  $U_e$ . Beyond,  $U_e$  the bed begins a regular expansion as a response to the mutual action of the gradual increase of the gas momentum and the magnetic cohesive forces between the magnetic particles. This process of uniform and bubble free expansion continues until the minimum fluidization velocity,  $U_{mf}$  is reached. At that transition velocity the stable bed breaks down and passes into the fluidized regime. The bed porosity at the onset of fluidized regime is the maximum porosity,  $\epsilon_{max}$  that the stabilized bed could attain.

Fig. 3 shows the effect of magnetic field intensity on  $\epsilon_{max}$  for different admixtures. It is evident that  $\epsilon_{max}$  increases as the magnetic field intensity,  $B$  increases. In addition,  $\epsilon_{max}$  decreases as the nonmagnetic fraction in the admixture increases. Fig. 4 reveals that  $\epsilon_{max}$  increases from 0.46 to 0.6 as  $B$  increases from 20 to 60 m T. In

addition,  $\epsilon_{max}$  decreases from 0.6 to 0.47 as the fraction of the nonmagnetic fraction increases from 0 to 73% when  $B$  equal 60 m T.

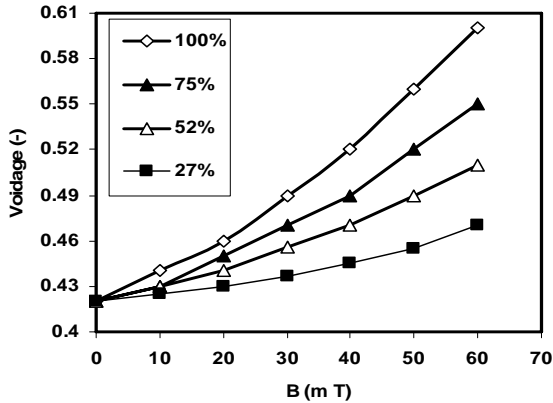


Fig. 3 The effect of magnetic field intensity on the maximum porosity of the stabilized bed,  $\epsilon_{max}$  for different admixture compositions

**B. Thermal Behavior of MSBs with Admixtures**

Fig. 4 shows the effect of gas velocity,  $U_g$  on the heat transfer coefficient,  $h$  for pure and different admixtures of magnetic particles and shale oil in the absence of magnetic field. It is evident that for certain admixture  $h$  increases as  $U_g$  increases until it reaches a maximum then starts to decrease when  $U_g$  exceeds  $U_{mf}$ . The heat transfer coefficient in a bed of shale oil particles reaches a maximum at lower gas velocity compared to the bed of the magnetic particles because its lower minimum fluidization velocity. In addition,  $h$  decreases as the mass fraction of the nonmagnetic particles increases for the same value of  $U_g$ .

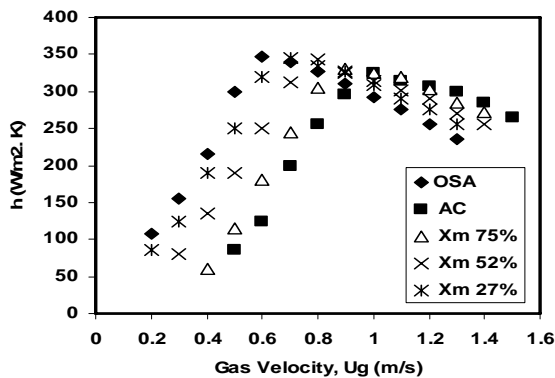


Fig. 4 Variation of heat transfer coefficient with gas velocity for different magnetic particles fractions in the absence of magnetic field

Fig. 5 shows the effect of gas velocity,  $U_g$  on the heat transfer coefficient  $h$  of a bed consisting of 100% mass fraction of the magnetic particles at various magnetic field intensities,  $B$ . The shape of these profiles depends on the bed structure under the effect of the magnetic field intensity and the gas velocity. In the absence of magnetic field ( $B = 0$  m T),  $h$  increases in a fast rate when  $U_g$  exceeds  $U_{mf}$  i.e., 0.574 m/s

in this case and the bed is the fluidized regime. The turbulence of the gas phase in the bed and that of the solid phase increases continuously with increasing  $U_g$ . This increase reaches a maximum and starts to decrease when the transfers to the slugging regime. The behavior of this profile is similar to that of conventional fluidized beds. Segregation of the bed particles was noticed in the fluidized regime according to their density. On the other hand, for  $B > 0$  m T, the bed is in a stabilized regime for  $U_g > 0.535$  m/s. In this flow regime the magnetic field usually suppresses the intensive movements of the solid phase mixing movements found in the fluidized beds, until it is completely impeded when  $B > 50$  m T. At that point the profile is similar to that of packed beds which is characterized by low  $h$  values compared to fluidized beds. The heat transfer coefficient in magnetized beds starts to increase when  $U_g$  exceeds  $U_{mf}$  and the bed transfers to a fluidized bed of strings or aggregates of particles. However, the values of  $h$  in this case are lower than those of particulate fluidization in the absence of magnetic field.

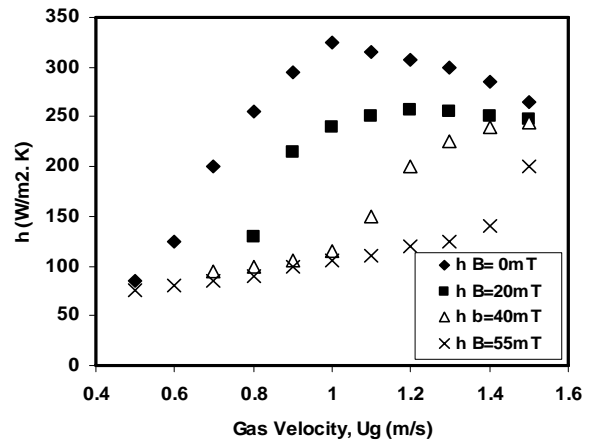


Fig. 5 Variation of heat transfer coefficient with gas velocity in a bed of pure magnetic particles for several of magnetic field intensities

The effect of magnetic stabilization on the heat transfer coefficient,  $h$  could be illustrated, by understanding the variation of the two  $h$  components i.e., particle convection and gas convection under the mutual effect of the magnetic field and gas velocity (1998). It illustrated above that one of the important consequences of the application of a magnetic field to a bed of magnetic particles is the increased bed height or porosity. This increase mainly depends on the intensity of the applied magnetic field,  $B$  and the gas velocity  $U_g$ . In this process the magnetic particles arrange themselves in the direction of the field lines. Accordingly, the interstitial gas velocity decreases and consequently gas turbulence decreases which implies reduction in the gas convection. On the other hand, the stabilized expanded bed is known to have a fluid like structure with local vibration of the solid particles. As a consequence, solid convection is higher than that in packed beds at the same gas flow rate but still lower than that of fluidized beds. The net effect on the two components is a net increase in  $h$  as reported in reference [14]. For this reason, the rate of  $h$  increase in the stabilized regime is higher than that in

fixed beds and the difference is more significant at  $B < 40$  m T. in m whereas the cell deposition rate increases.

Fig. 6 revealed one important behavior for  $h$  profiles under the effect of gas velocity at different values of  $B$ . It is the sudden jump in  $h$  values within a narrow gas velocity range near  $U_{mf}$ . This gas velocity range decreases as  $B$  increases. Ganzha and Saxena [14] referred this phenomenon to the increased particles immobility as  $B$  increases. However, this explanation could be more precise if it is connected to the bed porosity and  $U_{mf}$  under the effect of  $B$ . As mentioned in Figs. 2 and 3 both  $\epsilon_{max}$  and  $U_{mf}$  increases as  $B$  increases. This implies that the stability of the stabilized expanded bed near  $U_{mf}$  decreases as  $B$  increases. For this reason, a small increase in the gas velocity to the metastable structure of relatively low  $h$  values destroys it and transferred it to the fluidized state characterized by high  $h$  values.

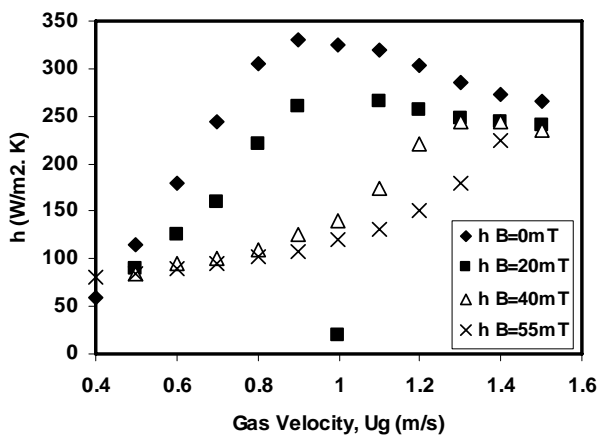


Fig. 6 Variation of heat transfer coefficient with gas velocity in a bed of admixtures of 75% magnetic particles for several of magnetic field intensities

It is shown above that the introduction of an admixture of magnetic and nonmagnetic particles strongly affects the hydrodynamics of the stabilized bed. Consequently, the thermal behavior of this bed should be influenced by the presence of the admixture compared to that of pure particles. Fig. 7 shows the effect of gas velocity on  $h$  at various  $B$  values for bed containing 75% mass fractions of the magnetic particles. Generally, these figures have the same behavior of Fig. 6 of the pure magnetic bed. However, it could be seen the heat transfer coefficient increases as the magnetic fraction decreases for all values of  $U_g$  and  $B$ . For example, when  $U_g$  equal 0.7 m/s and  $B$  equal 40 m T, the values of  $h$  are 100, 125 and 220 W/m<sup>2</sup>.K corresponding to magnetic fractions of 75, 52 and 27%, respectively. This behavior is attributed to the fact that as the nonmagnetic fraction in the bed increases, the effect of the magnetic field on the bed decreases and the mobility of these particles increases as the gas velocity increases. Accordingly, this enhances the heat transfer coefficient. The overall behavior of the profiles in Fig. 6 is similar to that shown in Fig. 5 where the mass fraction is still high. However, in cases when the magnetic fraction becomes low other unpublished results reveal that the profiles before  $U_{mf}$  are similar to those of a bed of nonmagnetic particles. In

this case, beyond  $U_{mf}$ , results show that the heat transfer coefficient increases as  $B$  increases. This behavior could be referred to the fact that as  $U_g$  increases beyond 1 m/s, the convective gas component of  $h$  is small due to the presence of large gas bubbles. In contrast, as  $B$  increases the magnetic particles start to arrange and suppress large bubble formation and as a consequence the convective gas component of  $h$  increases.

The variation of  $h$  with gas velocity,  $U_g$  in beds of different admixtures of magnetic and nonmagnetic and under the effect of constant magnetic field i.e., 40 m T, respectively is shown in Fig. 7. It is revealed in Fig. 7 that  $h$  increases as  $U_g$  increases as the magnetic fraction decreases. In addition, the data clearly indicate that each profile represents the variation of  $h$  in three subsequent regimes i. e., the packed, expanded stabilized and fluidized bed. This behavior is similar to that shown in Fig. 6 and could be explained in the same manner.

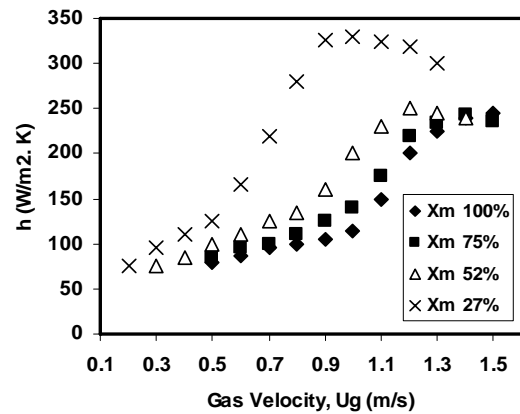


Fig. 7 Variation of heat transfer coefficient with gas velocity, in beds of different admixtures and under the effect of constant magnetic field intensity, a- 40 m T, b- 55 m T

Previously Ganzha and Saxena [14, 15] presented the following empirical to relate Nusselt number,  $Nu$  to Reynolds numbers,  $Re$  in the stabilized regime of a magnetically stabilized bed consisting of pure dense and relatively light magnetic particles, respectively:

$$Nu = 0.116Re^{0.8} + 5.67 \quad (7)$$

$$Nu = 1.04Re^{0.575} (B/B_s)^{-0.092} \quad (8)$$

where  $B_s$  is the saturation magnetic field intensity, m T Based on the results in the present investigation, equation 15 is modified to describe the effect of the presence of nonmagnetic fraction in the admixture. The following equation was obtained:

$$Nu = 1.95Re^{0.525} (B/B_s)^{-0.092} e^{-.66X_M} \quad (9)$$

This equation which is valid for the parameters ranges of  $20 < B$  (m T)  $< 45$ ,  $0.5 < U_g$  (m/s)  $< 1.3$  and  $0.25 < X_M < 0.75$  can be used to select the optimum operating conditions that give the highest heat transfer coefficient in the stabilized bed without forcing the bed particles to be segregated.

Segregation of the bed particles usually starts after bed fluidization. This drawback of beds consisting of admixtures

of magnetic and nonmagnetic particles could be minimized if the difference in the density of these particles is not high, the mass fraction of the magnetic particles is relatively high i.e., > 50% and the bed operates in the stabilized regime. In this case the magnetic particles form sufficiently stable and rigid network or "Bacon structure", which houses the nonmagnetic particles. Otherwise, if the density difference is large, and the mass fraction is low i.e., < 50%, the stabilized bed will not be rigid enough to keep the non magnetic particles and these will float at the top of the magnetic bed (1998).

## REFERENCES

- [1] Z. Al-Qodah "Hydrodynamic behavior of magneto air-lift column in a transverse magnetic field," *Can J. Chem. Eng.* Vol. 78, pp. 458-467, 2000.
- [2] M. Holger "Heat transfer between gas fluidized beds of solids particles and the surfaces of immersed heat exchanger elements: Part I," *Chem. Eng. Process*, Vol. 18, pp. 157-198, 1984.
- [3] J. C. Perkle, P. A. Ruziska, L. J. Shulik "Circulating magnetically stabilized bed reactors," *Chem. Eng. Commun.* Vol. 67, pp. 89-109, 1988.
- [4] M. V. Filippov "The Effect of a Magnetic Field on a Ferromagnetic Particle Suspension Bed," *Prik. Magnet Latv. SSR*, Vol. 12, pp. 215-220, 1960.
- [5] Y. A. Liu, R. K. Hamby, R. D. Colberg "Fundamental and Practical Developments of Magneto Fluidized Beds: a Review," *Powder Technol.* Vol. 64, pp. 3-11, 1991.
- [6] Z. Al-Qodah, M. Al-Busoul, M. Al-Hassan "Hydro-thermal behavior of magnetically stabilized fluidized beds," *Powder Technology* Vol. 115, pp. 58-67, 2001.
- [7] H. Holopainen (1991) "Experience of oil shale combustion in ahlistorm pyroflow CFB-boiler, *Oil Shale* 8: 194- 205, 1991.
- [8] R. E. Rosensweig "Fluidization: hydrodynamic stabilization with a magnetic field," *Science*, Vol. 204, pp. 57-59, 1979.
- [9] P. X. Thivel, Y. P. Gontier Boldo, A. Berns "Magnetically stabilized fluidization of a mixture of magnetic and non-magnetic particles in a transverse magnetic field," *Powder Technology*, Vol. 139, pp. 52-257, 2004.
- [10] J. Arnaldos, J. Casal, A. Lucas, L. Puigjaner "Magnetically stabilized fluidization: modeling and application to mixtures," *Powder Technology*, Vol. 44, pp. 57-62, 1985.
- [11] W. Y. Wu, K. L. Smith, S. C. Saxena "Rheology of a magnetically stabilized bed consisting of mixtures of magnetic and non-magnetic particles," *Powder Technology*, Vol. 91, pp. 181-187, 1979.
- [12] W. Y. Wu, A. Navada, S. C. Saxena "Hydrodynamic characteristics of a magnetically stabilized air fluidized bed of an admixture of magnetic and non-magnetic particles," *Powder Technology*, Vol. 90, pp. 39-46, 1997.
- [13] J. Arnaldos, L. Puigjaner, J. Casal "Heat and mass transfer in magnetically stabilized fluidized beds" In: K. Ostergaard and A. Sorensen, Editors, *Proceedings of Fifth Engineering Foundation Conference on fluidization, Fluidization V*, eds K. Ostergaard and A. Sorensen pp. 425-432, 1989.
- [14] V. L. Ganzha, S. C. Saxena "Heat-transfer characteristics of magneto fluidized beds of pure and admixtures of magnetic and nonmagnetic particles," *Int. J. Heat Mass Transfer*, Vol. 41, pp. 209-218, 1998.
- [15] Z. Al-Qodah, M. Al-Busoul "The effect of magnetic field on local heat transfer coefficient in fluidized beds with immersed heating surface," *Journal of Heat Transfer (ASME)*, Vol. 123, pp. 157-161, 2001.
- [16] Z. Al-Qodah, V. Evanova, E. Dobрева, I. Penchev, J. Hristov, R. Petrov "Non-porous Magnetic Support for Cell Immobilization," *J. Fer. Bioeng.* Vol. 71, pp. 114-117, 1991.
- [17] J. S. M. Botterill *Fluidized Bed Heat Transfer*, Academic Press, New York, 1975.
- [18] V. A. Girenko, J. Y. Hristov 2nd South-East European Symposium on FBC, in: S. Okada (Ed.), *Yugoslav Society of Heat Transfer Engineers, Arandjelovac, Yugoslavia*, p. 429, 1999.
- [19] Z. Al-Qodah, M. Al-Hassan "Phase holdup and gas-to-liquid mass transfer coefficient in magneto stabilized G-L-S airlift fermenter," *Chemical Engineering Journal*, vol. Vol. 79, pp. 41-52, 2000.